

Dimension dependence of the conductance distribution in the non-metallic regimes

Peter Markos

Institute of Physics, Slovak Academy of Sciences, Dúbravská cesta 9, 842 28 Bratislava, Slovakia

The conductance distribution $P(g)$ in disordered three-dimensional systems in the critical and insulating regimes is calculated numerically and compared with $P(g)$ of weakly disordered quasi-one-dimensional systems. Although both systems exhibit similar transport properties, their conductance distributions differ quantitatively. We explain this difference by analysis of the spectrum of transfer matrix. Our numerical data confirm that the statistics of the conductance is consistent with the one-parameter scaling also in the strongly localized regime.

PACS numbers: 71.30.+h, 71.23.-k, 72.15.Rn

I. INTRODUCTION

Our understanding of the metal-insulator transition (MIT) in disordered solids is based on the scaling theory of localization¹. We believe that MIT is universal. It means that the system-size dependence of any quantity, say conductance g , is determined only by one parameter. The validity of the one-parameter scaling was tested and confirmed in the neighborhood of the critical point by various numerical simulations on quasi-one-dimensional (Q1D) system $s^{2,3}$. However, a detailed analytical theory of MIT is still missing. Their formulation is complicated also by absence of the self-averaging of the conductance in disordered systems at zero temperature⁴. Complete description of transport properties requires therefore a detailed analysis of the conductance distribution $P(g)$. Such theory exists only in the weak disorder limit. The weak disorder expansion⁵, Doroхов-Mello-Pereyra-Kumar equation (DMPK)⁶, and the random matrix theory (RMT)^{7,8} provide us with entire quantitative description of the transport statistics. However, critical regime never appears in the weak disorder limit.

For the critical regime, analytical results for the conductance statistics were derived only in dimensions slightly above the lower critical dimension $d = 2 + \epsilon$ with $\epsilon \rightarrow 0$ ^{9,10}. These cannot be extrapolated to three-dimensional systems ($\epsilon = 1$)¹¹. Our information about the critical regime in 3D systems is therefore based only on numerical simulations. The shape of the conductance distribution at the critical point was analyzed^{11,13,17} and one-parameter scaling of the mean conductance was numerically proven in¹⁸.

Recently, an attempt has been made to obtain relevant information about the critical regime from studies of the weakly disordered Q1D system $s^{20,21}$. Although Q1D systems do not exhibit critical phenomena (corre-

lation length never diverges) their transport properties resemble that observed in 3D systems: (1) in the metallic regime when the system length L_z is shorter than the localization length, both RMT and the DMPK equation predict that $P(g)$ in Q1D systems is Gaussian with a constant, disorder independent width. This was numerically observed also for squares (2D)¹⁹ and cubes (3D)^{7,12,11}. Only the variance of conductance depends on the dimension⁵. (2) In the limit of very long system length, $L_z \rightarrow \infty$, Q1D samples become insulating, in spite of weak disorder. RMT predicts that the distribution of $\log g$ is Gaussian and $\text{var} \log g = 2h \log g^2$. Log-normal distribution was observed also in 2D and 3D strongly disordered system $s^{22,23}$. The dimension-dependence of the variance $\text{var} \log g$ is, however, not understood. (3) In the intermediate regime, where $hgi \approx 1$, analytical relation for the conductance distribution can be obtained^{20,21}. Its shape is similar to that obtained numerically at the critical point of MIT¹⁶.

In this paper we discuss the differences between the conductance distribution for Q1D weakly disordered systems and for 3D cubes. As the metallic limit is already good understood both analytically^{6,8,27} and numerically^{11,12} we concentrate to the critical regime ($hgi \approx 1$) and the strongly localized regime ($hgi \ll 1$). Although the distributions are qualitatively similar in each transport regime, quantitative differences will be found. We show that statistics of the conductance depends on the dimension in the critical and even in the localized regime. This must be taken into account in the entire description of the transport. Our analysis of the statistical properties of parameters z , which are defined by Eq. (2) below, confirms the validity of the one-parameter scaling theory in the insulating regime.

In Section 2 we describe the model we use. Section 3 presents numerical data for the conductance distribution in the intermediate (critical) regime. The shape of the distribution in the three-dimensional localized regime is studied in detail in Section 4.

II. THE MODEL

We consider Anderson model defined by the Hamiltonian

$$H = \sum_n W_n \sum_j |n\rangle \langle j| + \sum_{\langle n, n^0 \rangle} J_{nn^0} |n\rangle \langle n^0| \quad (1)$$

where n counts the sites in d -dimensional lattice and nn^0 are nearest-neighbor sites. The size of the lattice is either

L^d ($d = 2;3$) or L^{d-1} L_z . Random energies ϵ_n are distributed with the box distribution J_n $j = 1,2$ and W is the strength of the disorder.

Our analysis of the conductance distribution is based on the Landauer formula for the conductance²⁵

$$g = \text{Tr } t^y t = \frac{1}{N} \sum_{i=1}^N \cosh^2(z_i/2) \quad (2)$$

In (2), t is the transmission matrix, and the parameters z_i , $i = 1,2,\dots,N$, parameterize the eigenvalues of $t^y t$. In the limit $L_z \gg L$, parameters z converge to Lyapunov exponents of the transfer matrix. N is the number of open channels²⁶.

According to (2), statistics of the conductance is completely determined by statistical properties of the parameters z . It is well known that in weakly disordered systems the spectrum of z is linear

$$z_i / i \quad (3)$$

independently on dimension and shape of the sample^{6;7}. The linear behavior (3) can be derived also from the random matrix model²⁴ and was used in Ref.²⁷ to prove of the universality of conductance fluctuation⁵.

It is important to mention that weakness of the disorder is not only necessary but also sufficient condition for the linear form of the spectra (3). Relation (3) holds therefore for any weakly disordered Q1D systems independently on the system length^{2;7;8;24}. This is not true when disorder increases. Thus, we have numerically proven that

$$z_1^{d-1} / i \quad W = W_c: \quad (4)$$

at the critical point of MIT in dimension $d = 3$ and 4 . Relation (4) holds for both Q1D²⁸ and 3D¹¹ systems. In 3D, it enables us to understand the dimension-dependence of the conductance distribution at the critical point^{15;16}.

The form of the spectra of z for strongly disordered systems is known for the Q1D samples²⁹. An attempt was made to study z for 2D and 3D strongly disordered system^{22;23}. We present here much more accurate data for parameters z , which enable us to estimate the contribution of higher channels to the conductance.

III. CONDUCTANCE DISTRIBUTION IN THE INTERMEDIATE (CRITICAL) REGIME

Three-dimensional Anderson model with a box distributed disorder exhibits MIT at the critical point $W_c = 16.5$. We calculated the conductance distribution for ensembles of three-dimensional cubes with disorder $10.6 < W < 21.5$. The system size was $8 \times 8 \times 8$ which is large enough to exhibit quantitative properties of the conductance distribution. Calculated shape of $P(g)$ is compared with the conductance distribution for weakly

disordered Q1D systems of the size $8^2 \times L_z$. The disorder $W = 4$ assures the existence of the metallic regime for short L_z , $L_z < 100$. The localized regime appears when L_z exceeds 250. Tuning the length L_z we find for each 3D ensemble the corresponding Q1D ensemble with the same mean conductance.

A comparison of the conductance distribution of 3D and Q1D systems is presented in Figures 1, 2 and 4. In the metallic regime, when $hgi > 1$, $P(g)$ is Gaussian in both 3D and Q1D geometry, as supposed (Fig. 1a). The width of the distribution is universal, independent on the system size. It depends only on the system shape, and is slightly smaller for Q1D than for 3D systems, in agreement with theoretical results^{5;27}.

Figures 1 (b-e) present the shape of $P(g)$ in the critical regime, when $hgi \approx 1$. We know that $P(g)$ for 3D systems becomes non-analytical at $g = 1$ and decreases exponentially when $g > 1$ ^{15;16}. The same is true also for Q1D systems in the intermediate regime^{20;21}. $P(g)$ decreases for $g > 1$ much faster than predicted theoretically²⁰. The exponential decrease in Q1D is even faster than that in 3D systems. This is because for a given hz_1 the difference $hz_2 - z_1$ is much smaller in 3D than in Q1D, as follows from the comparison of (3) with (4). Higher channels have therefore a better chance to contribute to the conductance in 3D than in Q1D.

Figure 2 presents the conductance distribution for 3D Anderson model at the critical point ($W_c = 16.5$) and for 2D and Q1D systems with the same mean conductance. As supposed, 3D distribution possesses the longest tail, while two Q1D-distributions are almost identical. From the plot of the $P(\log g)$ (data not shown in the paper) we conclude that all four distributions are identical for small g . This is not surprise since the small- g behavior is determined completely by the distribution of z_1 , which is the same in all systems.

The quantitative difference between the conductance distribution for cubic and Q1D systems is measured by the integral

$$I(1) = \int_1^{z_1} P(g) dg \quad (5)$$

In figure 3 we plot $I(1)$ as a function of the mean conductance hgi for various geometrical shapes of systems. For Q1D systems, we calculated both $L \times L_z$ and $L^2 \times L_z$ ($L_z \gg L$). The data lay on the same curve. This is no surprise since the spectrum of z is linear in both systems. A similar universality was found in 2D system. Here, we either increase disorder with constant system size or increase the size of square samples keeping disorder constant. As supposed, the data for 3D and 2D systems scales independently.

The figure 4 compares $P(\log g)$ for 3D and Q1D systems in localized regime. It confirms that $P(\log g)$ converges to Gaussian both for 3D and Q1D systems. The distribution for Q1D systems is much broader than that for 3D. While the shape of $P(\log g)$ in weakly disor-

dered Q 1D systems can be obtained analytically^{7;24}, distribution for 3D systems is known only from numerical simulations^{22;23} and deserves more detailed analysis.

IV. STRONGLY LOCALIZED REGIME

In the insulating regime all z increase linearly with the system length. The length-dependence of z_1 determines the localization length

$$z_1(L) = \frac{2L}{\pi} + \text{const} \quad (6)$$

(For Q 1D systems, L should be replaced by L_z).

The knowledge of the spectrum of parameters z is important also in the insulating regime. As mentioned above, the spectrum of z remains linear in weakly disordered Q 1D systems^{7;24} so that $z_2 = 2z_1 - z_1$. Contrary to Q 1D systems, we find that the difference $hz_2 - z_1$ increases only logarithmically with the system size for 2D systems (Figure 5):

$$hz_2 - z_1 \sim \log L \quad \text{2D systems} \quad (7)$$

The same logarithmic behavior was found also in the 2D systems with spin-orbit scattering (data are not presented here).

In 3D systems we find that the differences $hz_2 - z_1$ and $hz_3 - z_1$ do not depend on the system size in the strongly localized regime:

$$hz_2 - z_1 \sim \text{const} \quad \text{3D systems} \quad (8)$$

In Figure 6 we present the z_1 -dependence of the difference $hz_2 - z_1$ for the 2D and 3D systems. For z_1 large enough, data scale to the same curve, confirming the one-parameter scaling. More important, data prove that the spectrum of the transfer matrix depends on the dimension of the sample in the localized regime.

Figure 7 presents the z_1 -dependence of the differences $hz_i - z_1$ for $i = 2; 3; 4$ and 5. Although the convergence is worse for higher differences, the saturation to the z_1 -independent constant is clearly observable as z_1 increases.

Due to (8), the contribution of the second channel is nonzero whichever is the contribution of the first one. This contribution, however, gives only small correction to the first channel contribution $h \log g = \log 4 - hz_1$. Nevertheless, it is interesting to test how the contributions of the higher channels influence the statistical properties of the conductance. We found that apart the shift of the mean value the distribution $P(-\log g)$ and the distribution $P(z_1)$ are almost identical.

Although the absolute value of the conductance changes only slightly due to the contribution of higher channels, the present effect influences the variance of the $\log g$. Indeed, the small difference $z_2 - z_1$ causes that z_1 is confined from above: the probability to find $z_1 \gg hz_1$ is much less in the 3D than in the Q 1D. The width of

the distribution of z_1 and of $\log g$ is therefore narrower in 3D than in the Q 1D. This agrees with numerical data presented in Figure 4. Note also an asymmetry of the distribution: the probability to find $\log g = h \log g +$ is higher than the probability to find $\log g = h \log g -$ (> 0).

To support one-parameter scaling by more quantitative arguments we analyzed also statistical properties of the parameters z . Contrary to weakly disordered Q 1D systems, we have to take into account also mutual correlations of z_1 and higher z in 3D. It is therefore not clear in advance, whether or not the one-parameter scaling theory is valid in this regime. However, Figure 6 shows that the differences $hz_i - z_1$ are unambiguous functions of hz_1 . Validity of the one-parameter scaling in the localized regime is confirmed also by the data in Figure 5 which shows that $\text{var } z_1$ is an unambiguous function of the mean value hz_1 in 2D even when disorder is strong. The same seems to hold also for 3D systems (Figure 8). In Figure 8 we present also the $h \log g$ -dependence of $\text{var } \log g$. In the last case we find deviations from scaling only when the localization length becomes comparable with inter-atomic distance (~ 1). We analyzed also systems with non-zero Fermi energy. This was motivated by Ref.³⁰, where separate $\text{var } z$ vs hz_i relations were found in systems with different Fermi energy. Our present data, however, scale to the same curve as that for the zero Fermi energy (Figure 8). However, we cannot guarantee that more detailed statistical analysis will not show small deviations from the one-parameter scaling, similar to that observed in one-dimensional systems³⁰.

V. CONCLUSION

We have shown numerically that the shape of the conductance distribution depends on the system dimension when the system leaves metallic regime. Qualitative explanation of this difference is based on the known spectra of the parameters z . In weakly disordered quasi-one-dimensional systems the spectrum of z is linear independently on the dimension and the system length. However, in the cubic d-dimensional samples the spectrum depends on the dimension of the system when the disorder increases.

We presented and compared the conductance distributions for Q 1D and 3D systems in the intermediate (critical) regime. For both of them we found non-analytical behavior in $g = 1$ and exponential decrease of $P(g)$ for $g > 1$. The distributions differ only quantitatively.

We have shown for the first time that the differences $hz_2 - z_1$ increase logarithmically with the system size in two-dimensional strongly disordered systems. In three-dimensional strongly disordered systems the differences $hz_2 - z_1$ and $hz_3 - z_1$ are constant and independent on the system size and on the strength of the disorder. This agrees with previous results²⁹. The contributions to

the conductance from the first, the second and higher channels have therefore the same system-size dependence $\exp -z$. Although the contribution of higher channels to the mean conductance is small, the shape of the spectra of z influences strongly the form of the distribution of the $\log g$, which becomes narrower in 3D than in the weakly disordered quasi-one dimensional systems. The one-channel approximation is therefore not sufficient for the entire description of the insulating regime in three dimensions.

Our numerical data confirm that z_2, z_3 together with $\text{var } z_1$ are unambiguous functions of z_1 . We believe therefore, that, in spite of the non-linearity of the spectrum of z , the random matrix theory can be generalized to the description of the non-metallic systems^{31,29}. Such a generalization would approve applicability of the one-parameter scaling theory both to the critical and the strongly insulating regime.

This work was supported by Slovak Grand Agency VEGA, Grant n. 2/7174/20. Numerical data were partially collected using the computer Origin 2000 in the Computer Center of the Slovak Academy of Sciences.

* E-mail address: m.arkos@savba.sk

- ¹ E. Abraham s, P. W. Anderson, D. C. Licciardello and T. V. Ram akrishnan, Phys. Rev. Lett. 42, 673 (1979)
- ² A. M acK innon and B. K ram er, Phys. Rev. Lett. 47, 1546 (1981)
- ³ B. Bulka, B. K ram er and A. M acK innon, Z. Phys. B 60, 13 (1985); B. K ram er, K. Broderik, A. M acK innon and M. Schreiber, Physica A 167, 163 (1990); A. M acK innon, J. Phys.: Condens. M att. 6, 2511 (1994); K. Slevin and T. Ohtsuki, Phys. Rev. Lett. 82, 382 (1999); P. Cain, R. A. Rom er and M. Schreiber, Ann. Physik. (Leipzig) 8, SI-33 (1999)
- ⁴ P. W. Anderson, D. J. Thouless, E. Abraham s and D. S. Fisher, Phys. Rev. B 22, 3519 (1980); B. Shapiro, Phys. Rev. Lett. 65, 1510 (1990)
- ⁵ P. A. Lee, A. D. Stone and H. Fukuyam a, Phys. Rev. B 35, 1039 (1987)
- ⁶ O. N. Dorokhov, JEPT Letter 36, 318 (1982); P. A. M ello, P. Pereyra and N. Kum ar Ann. Phys. (NY) 181, 290 (1988)
- ⁷ J.-L. P ichard, in Quantum Coherence in Mesoscopic Systems, Ed. by B. K ram er, NATO ASI Ser B 254 369 (1991)
- ⁸ C. W. J. Beenakker and R. R a jaei, Phys. Rev. B 49, 7499 (1994)
- ⁹ B. L. Altshuler, V. E. Kravtsov and I. V. Lerner, Soviet JETP 64, 1352 (1986); JETP Lett. 43, 441 (1986);
- ¹⁰ B. Shapiro and A. Cohen, Int. J. Mod. Phys. B 6, 1243 (1992)
- ¹¹ P. M arkos and B. K ram er, Phil. Mag. B 68, 357 (1993)
- ¹² N. G iordano, Phys. Rev. B 38, 4746 (1988)
- ¹³ P. M arkos, Europhys. Lett. 26, 431 (1994)
- ¹⁴ K. Slevin and T. Ohtsuki, Phys. Rev. Lett. 78, 4083 (1997);
- ¹⁵ ibid 82, 689 (1999); C. M. Soukoulis, Xiaosha Wang, Q uin ing Li and M. M. Sigalas, Phys. Rev. Lett. 82, 688 (1999)
- ¹⁶ P. M arkos, Phys. Rev. Lett. 83, 588 (1999)
- ¹⁷ M. Ruhlander, P. M arkos and C. Soukoulis, cond-mat/0104394
- ¹⁸ Xiaosha Wang, Q uin ing Li and C. M. Soukoulis, Phys. Rev. B 58, 3576 (1998)
- ¹⁹ K. Slevin, P. M arkos and T. Ohtsuki, Phys. Rev. Lett. 86, 3594 (2001)
- ²⁰ Providing that system size L is smaller than localization length.
- ²¹ K. A. M uttalib and P. W o l e, Phys. Rev. Lett. 83, 3013 (1999)
- ²² A. Garcia-Mart in and J. J. Saenz, Phys. Rev. Lett. 87, 116603 (2001)
- ²³ B. K ram er and M. Schreiber, J. non-cryst. Solids 114, 330 (1989)
- ²⁴ P. M arkos and B. K ram er, Ann. Physik. (Leipzig) 2, 339 (1993)
- ²⁵ K. A. M uttalib, Phys. Rev. Lett. 65, 745 (1990)
- ²⁶ R. Landauer, IBM Res. Dev. 1, 223 (1957); E. N. Econom ou and C. Soukoulis, Phys. Rev. Lett. 46, 618 (1981); D. S. Fisher and P. A. Lee, Phys. Rev. B 23, 6851 (1981);
- ²⁷ T. Ando, Phys. Rev. B 44, 8017 (1991);
- ²⁸ I. Ym ry, Europhys. Lett. 1, 249 (1986)
- ²⁹ P. M arkos and M. Henneke, J. Phys.: Condens. M att. 6, L765 (1994); P. M arkos, NATO ASI Ser. E 291, 99 (1995)
- ³⁰ P. M arkos, J. Phys.: Condens. M att. 7, 8375 (1995)
- ³¹ K. Slevin and J. B. Pendry: J. Phys.: Condens. M att. 2, 2821 (1990)
- ³² Y. Chen, H. E. M. Ismail and K. A. M uttalib, J. Phys.: Condens. M att. 4, L417 (1992)

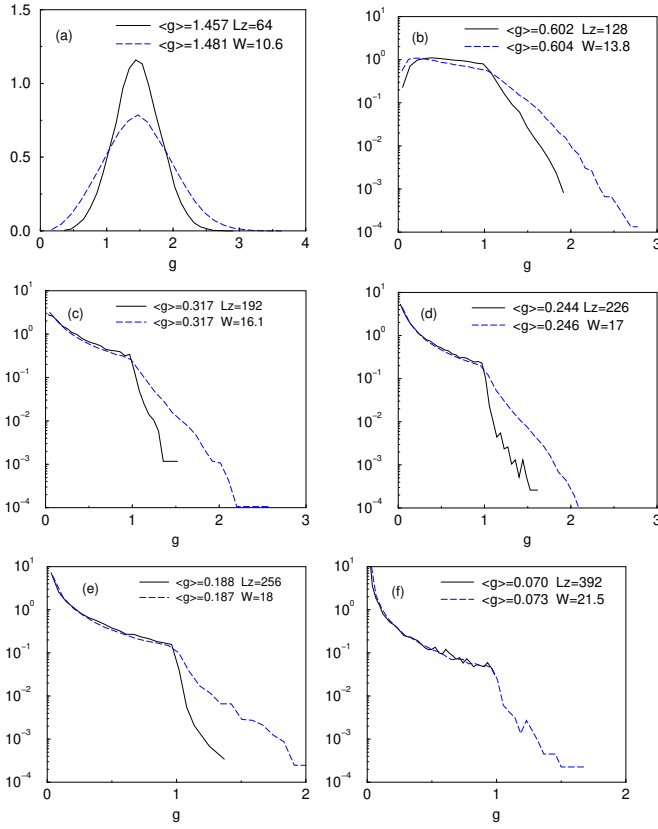


FIG. 1. Conductance distribution $P(g)$ for cubic samples $L \times L \times L$ with $L = 8$. Disorder increases from $W = 10.6$ (metallic regime, $\langle g \rangle = 1.481$) to $W = 21.5$ (insulator, $\langle g \rangle = 0.073$). Critical disorder is $W_c = 16.5$ and mean conductance at the critical point is $\langle g \rangle_c = 0.28$. For each value of the disorder, we plot $P(g)$ (dashed line) and compare it with the conductance distribution for weakly disordered Q1D system which possesses the same mean conductance (solid line). Size of Q1D system is $L^2 \times L_z$ with $L = 8$, disorder $W = 4$ and length is tuned to get required $\langle g \rangle$. Fixed boundary conditions were applied in x and y directions. 10^5 samples were collected from most statistical ensembles. (a) – metallic regime, $P(g)$ is Gaussian for both cubic and Q1D geometry. Distributions differ from each other only in their width: $\text{var } g_{3D} = 0.27$ and $\text{var } g_{Q1D} = 0.12$. This agrees with theoretical data (0.31 and 0.133 for 3D and Q1D, respectively⁵). Figures (b) – (e) present $P(g)$ in the critical regime: $\langle g \rangle = 1$. The main difference between conductance distributions is observable in region $g > 1$. (f) shows the conductance distributions in the insulating regime. Note that there are no Q1D sample with conductance $g > 1$ while $P(g)$ for cubes still possesses tail up to $g = 1.5$.

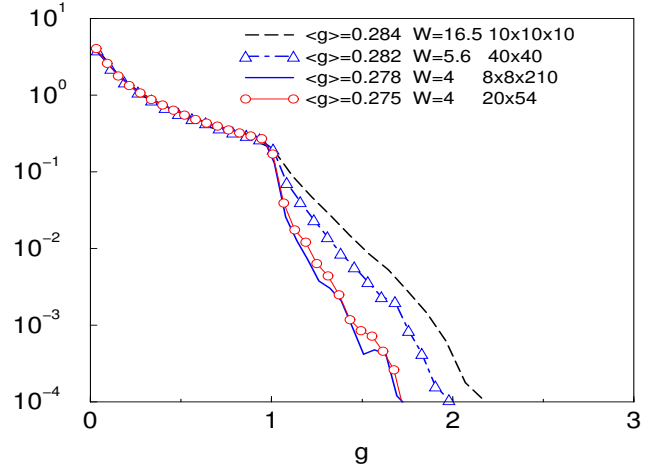


FIG. 2. Critical conductance distribution for 3D Anderson model (dashed line) and conductance distribution for square and quasi-one dimensional systems $L \times L_z$ and $L^2 \times L_z$ which have approximately the same mean conductance. As it is supposed, the quasi-one dimensional systems have the identical distributions.

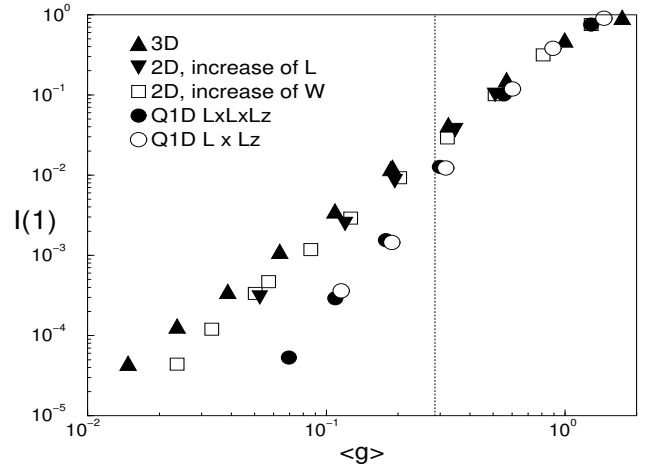


FIG. 3. Integral $I(1) = \int_1^{R_1} P(g) dg$ as a function of $\langle g \rangle$ for different geometrical shapes of samples. Dotted vertical line indicates mean critical conductance for 3D Anderson model. $I(1)$ decreases more quickly for Q1D systems than for squares and cubes. For the quasi-one dimensional systems data for systems $L \times L_z$ and $L^2 \times L_z$ scale to one curve. This is caused by the universal (linear) spectrum of z . Data for squares and cubes scale differently due to the dimension dependence of spectrum of z .

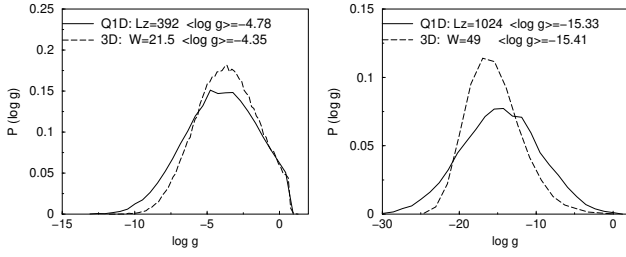


FIG. 4. (a) Distribution $P(\log g)$ for 3D and Q1D systems displayed in Figure 1 (f). Note that although systems have the same $h g_i$, they differ in $h \log g_i$. This indicates that mean conductance is not relevant parameter in the insulating regime. The width of the distribution is larger for Q1D system, (var $\log g = 6$ for the Q1D system, and 4.33 for 3D system). (b) the same for 3D and Q1D systems with $h \log g_i = 15.3$. Different width of distribution is clearly visible: var $\log g = 25.66$ for the Q1D system, and only 12.6 for 3D system. This is consistent with previous numerical results⁷.

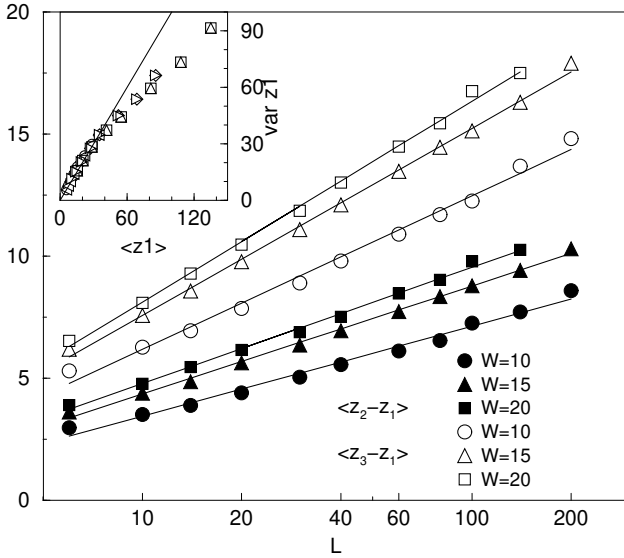


FIG. 5. System-size dependence of the differences $h z_2 - z_1$ and $h z_3 - z_1$ for 2D orthogonal systems. Three different values of disorder were used. Solid lines are logarithmic fits. 2D symplectic systems exhibit the same logarithmic dependence. Inset: Plot of $\text{var } z_1$ vs. $h z_1$.

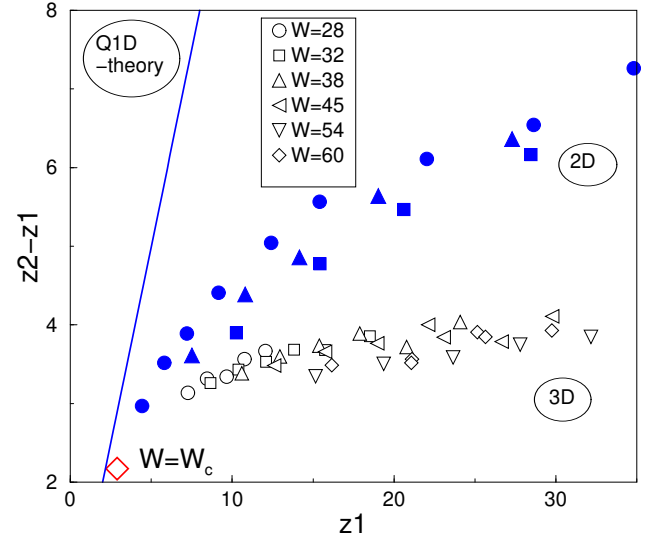


FIG. 6. $h z_1$ i-dependence of difference $h z_2 - z_1$ for 2D (full symbols) and 3D (open symbols) disordered systems. Solid line is the theoretical prediction $h z_2 - z_1 = h z_1$ for the Q1D weakly disordered systems.

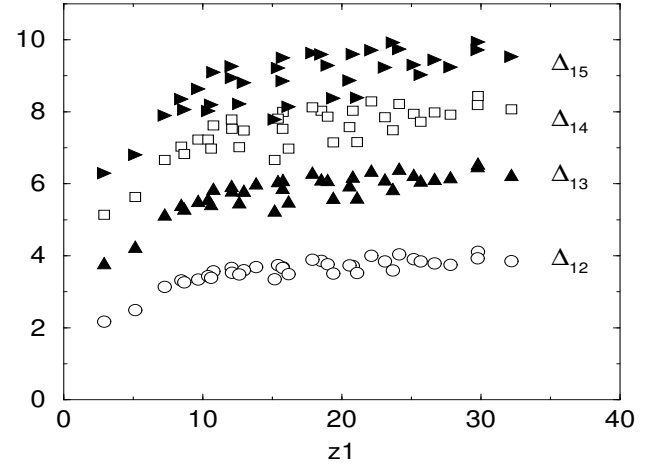


FIG. 7. z_1 -dependence of the differences $h z_1 - z_1$ for $i = 2, 3, 4$ and 5 . Disorder $W = 28, 32, 38, 45, 54$ and 60 , system size $L = 6, 8, \dots, 16$. Data for $W = 16.5$ and $W = 20$ ($L = 8$) are also presented to show how s increase from their "critical" values ($W = W_c$). For large z_1 , they converge to constant, which do not depend neither on the system size nor on the disorder.

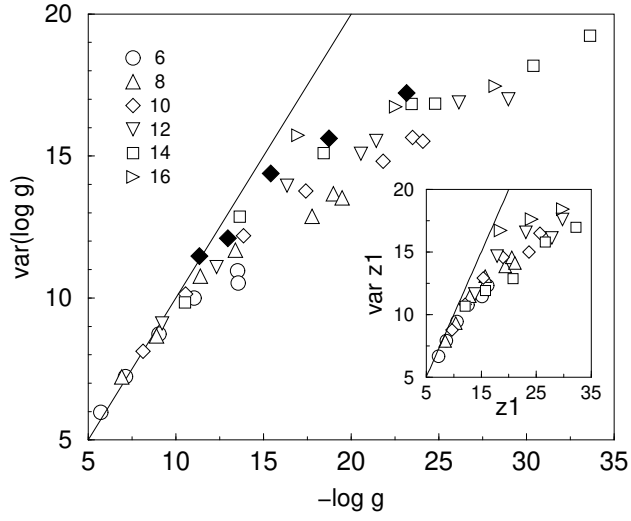


FIG. 8. $\text{var} \log g$ vs $-\log g$ for various W and L . Solid line is linear dependence $\text{var} \log g = -\log g$. Data lie on the same curve with exception of some points for $L = 6$ and 8 , which represent systems with localization length smaller than inter-atomic distance. For completeness, we calculated also $\text{var} \log g$ for some systems with non-zero Fermi energy ($= 4.4$ and 2.5) with $L = 12$, full diamonds.